Consistency Tests for Binary VLE Data

Philip T. Eubank* and Brad G. Lamonte

Texas A&M University, Department of Chemical Engineering, College Station, Texas 77843-3122

J. F. Javier Alvarado

Instituto Tecnologico de Celaya, Depto. de Ingenieria Quimica, Celaya, C.P. 38010, Gto., Mexico

Many VLE data papers are published each year for binary systems at either constant temperature or constant pressure. This manuscript examines consistency checks via Gibbs−Duhem equations and finds most powerful a two-step method that (1) uses a combination of the liquid and vapor Gibbs−Duhem equations to first check the internal consistency of (P, y, x) at constant temperature or (T, y, x) at constant pressure and (2) then uses the liquid-side Gibbs−Duhem equation to check the liquid-phase activity coefficients in a test more familiar to most workers. A new graphical method is developed in conjunction with step 1. The role of the assumed gas-phase model is examined. The common problem of published data of the activity coefficient of the solvent falling slightly under unity upon approaching the pure solvent end on the familiar ln γ_i versus x_1 diagram is explained as an artifact of usual data reduction procedures but corrected by the present procedures.

Introduction

Many research articles are published each year containing low-pressure, vapor−liquid equilibrium (VLE) data for binary systems with the composition measured in one or in both phases. As clearly seen in the compilations of Hala et al. (1967, 1968) and of Gmehling and Onken (1990), about half of these data are taken at constant temperature (P, y, x) and about half at constant pressure (T, y, x), often near atmospheric pressure. The phase rule of Gibbs provides for two independent intensive variables so that when either the pressure P or the temperature T is fixed, the composition of the liquid x and of the vapor y cannot be changed without variation of T or P, respectively. Reviews of the many experimental methods have been given by Hala et al. (1967), Williamson (1975), Marsh (1978), Malanowski (1980), and very recently Raal (2000). Especially detailed reviews have been presented of the dynamic method (recirculating stills) by Hala et al. (1967) and of the static method by Marsh (1978).

Because the main objective of these experiments is to find the liquid-phase activity coefficients $\gamma_i(x, P, T)$ or, equivalently, the liquid-phase excess Gibbs energy, $g \equiv (G^E/RT)$, isothermal measurement of the three variables (P, y, x) or isobaric measurement of the three variables (T, y, x) provides the activity coefficients from the equilibrium relation

$$\hat{f}_i^{\mathrm{v}} = \hat{\phi}_i P y_i = \hat{f}_i^{\mathrm{l}} = \gamma_i P_i^{\sigma} \phi_i^{\sigma} (\mathrm{PC})_i x_i \qquad (1)$$

where $\hat{f}_i$ is the fugacity of component i in the vapor and liquid mixtures, $\hat{\phi}_i$ is the vapor-phase fugacity coefficient, ϕ_i^{σ} is the fugacity coefficient of pure i at its vapor pressure P_i^{σ}, and $(\mathrm{PC})_i$ is the pure liquid i Poynting Correction,

$$(\mathrm{PC})_i \equiv \exp\left[\int_{P_i^{\sigma}}^{P} (V_i^{\mathrm{L}}/RT)\, \mathrm{d}P\right] \cong \exp[\langle V_i^{\mathrm{L}} \rangle (P - P_i^{\sigma})/RT] \qquad (2)$$

where $\langle V_i^{\mathrm{L}} \rangle$ is the average liquid molar volume of pure i between the vapor pressure and the system (equilibrium) pressure P. Because the coefficients $\hat{\phi}_i$, ϕ_i^{σ}, and $(\mathrm{PC})_i$ can be evaluated separately, and the vapor pressure of pure i represents temperature, eq 1 can be viewed as connecting the measured variables of (P, T, y, x) to the activity coefficient γ_i.

In addition to eq 1, an independent Gibbs−Duhem equation can be written for each of the coexisting phases. These differential identities can be written in several alternate forms. Here we use

$$(y)\, \mathrm{d} \ln \hat{f}_1 + (1 - y)\, \mathrm{d} \ln \hat{f}_2 = [(V_{\mathrm{m}}^{\mathrm{v}})/RT]\, \mathrm{d}P - [H_{\mathrm{m}}^{\mathrm{v,res}}/RT^2]\, \mathrm{d}T \qquad (3)$$

for the vapor phase and either

$$(x)\, \mathrm{d} \ln \hat{f}_1 + (1 - x)\, \mathrm{d} \ln \hat{f}_2 = [(V_{\mathrm{m}}^{\mathrm{l}})/RT]\, \mathrm{d}P - [H_{\mathrm{m}}^{\mathrm{l,res}}/RT^2]\, \mathrm{d}T \qquad (4a)$$

or

$$(x)\, \mathrm{d} \ln \gamma_1 + (1 - x)\, \mathrm{d} \ln \gamma_2 = [(V^{\mathrm{E}})/RT]\, \mathrm{d}P - [H^{E}/RT^2]\, \mathrm{d}T \qquad (4b)$$

for the liquid phase. The superscript res denotes a residual property. These equations are written for a binary system with $y \equiv y_1$ and $x \equiv x_1$. In eq 4b, V^{E} and H^{E} are the excess volume and excess enthalpy, respectively. Normally, eqs 1, 3, and 4 would be independent, but in low-pressure VLE the vapor phase is assumed to be either a perfect gas mixture (PGM; $\hat{\phi}_i = 1$) or a second virial gas mixture

* Author to whom correspondence should be addressed. E-mail: p-eubank@tamu.edu.

10.1021/je9902692 CCC: $19.00
Published on Web 09/08/2000

(SVGM) where

$$\ln(\hat{\phi}_1) = (P/RT)[(B_{11}) + (1 - 2y)\delta_{12}];$$
$$(PV^{v}_{m}/RT) \equiv Z^{v}_{m} = 1 + (B_{m}P/RT);$$
$$B_{m} = yB_{11} + (1 - y)B_{22} + y(1 - y)\delta_{12};$$
$$H^{v,res}_{m} = P[B_{m} - T(dB_{m}/dT)] \quad (5)$$

and $\delta_{12} \equiv 2B_{12} - B_{11} - B_{22}$ plus $\ln \phi^{\sigma}_{i} = (P^{\sigma}_{i}B_{ii}/RT)$. Experimental values for both B_{ii} and B_{ij} can be found as a function of temperature for a variety of compounds in Dymond and Smith (1980). Even at high pressures for vapor mixtures that approximate an ideal solution, the fugacity coefficient ratio can be evaluated as $(\hat{\phi}_i) \cong (\phi)$, where these pure-component fugacity coefficients may be estimated from a corresponding states procedure such as the Lee−Kesler method (see Smith et al., 1996).

As in the case of creditable empirical activity coefficient models for the liquid phase (Abbott and Prausnitz, 1994), the vapor **model assumption** provides automatic compliance with the vapor-phase GD equation, eq 3. With the more general SVGM assumption, the equilibrium relation of eq 1 becomes (Van Ness and Abbott, 1982)

$$\ln \gamma_i = \ln[y_iP/x_iP^{\sigma}_{i}] + [(B_{ii} - \langle V^{L}_{i}\rangle)(P - P^{\sigma}_{i})/RT] + y^{2}_{j}(\delta_{ij}P/RT) \quad (6)$$

It is most important to understand that while eq 3 may be used in the development of other identities, it no longer provides a third independent equation (with eqs 4 and 6) now that a vapor model has been assumed. Indeed, many VLE experiments measure only the composition of one of the equilibrium phases and use the above equations to find the unmeasured composition. In so consuming the liquid-phase GD equation, their results were made consistent but without any independent test of the data itself (Van Ness, 1995). While it is more difficult to measure accurately the vapor-phase composition y compared to the liquid-phase composition x, it is also more difficult to calculate accurately y from bubble-point measurements of (P, x) (Sayegh and Vera, 1980) than in the reverse calculation, as shown in the next section. To provide $\gamma_i(x, P, T)$, we must know accurately x, so past data reduction methods have centered on the calculation of y, γ, and g from measurements of (P, x); an excellent understanding of these methods can be obtained by reading Sayegh and Vera (1980) followed by Van Ness (1995) with consideration for the articles referenced therein. When both y and x have been measured, then consistency tests are possible.

In recent years most VLE articles include measurement of both y and x due to (1) pressure from the thermodynamics community to allow consistency tests and (2) improvements in the accuracy of y from better vapor sampling techniques as well as improved GC analysis. For the static method, we consider that both y and x have been measured when the moles of each pure component are mixed to form the starting liquid and the composition y of the small amount of vapor formed is measured directly along with pressure and temperature; from an estimate of the volume of vapor, the amount of vapor is estimated, and thus x for the equilibrium liquid can be calculated from material balances. No GD equations have been used. Such static procedures starting with synthetic liquid mixtures can provide data of high accuracy, as demonstrated in the past 30 years by research groups led by H. C. Van Ness, K. N. Marsh, Buford Smith and J. Gmehling, among others. These procedures are similar to high-pressure VLE techniques reviewed by Eubank (1980).

Authors and reviewers of such data should be aware of the consistency tests afforded by the above equations, as demonstrated in the remainder of this article. Considerable care must be used in application of abbreviated forms of GD equations, such as the common integral test for activity coefficients, so that data are not declared inconsistent when, in fact, the problem lies with the test and not the data. The data should be treated as innocent until *proven* guilty. However, the reverse side of this comment is that few authors make all of the consistency tests outlined here, resulting in truly inconsistent measurements. What follows is a guide to proper applications of the GD equation with some familiar equations perhaps repackaged more conveniently and all in one place. We do not claim any really new equations but rather variations in their application to the data. With the publication of so many VLE data manuscripts in this journal and others, we hope to remind both authors and reviewers of GD constraints in the hope that these checks will be made before publication.

General Methodology

We have found utility in a two-step method that (1) uses a combination of the liquid and vapor Gibbs−Duhem equations to first check the internal consistency of (P, y, x) at constant temperature or (T, y, x) at constant pressure and (2) then uses the liquid Gibbs−Duhem equation to check the liquid-phase activity coefficients in a test more familiar to most workers. Both tests are based on eqs 4 and 6, and so it can be proven *theoretically* that when one is satisfied, so must be the other. However, we have found that, in dealing with real data, one test may be more sensitive in checking errors in a particular measured variable. For example, the first test is a more sensitive test of the correctness of the pressure and temperature measurements, as the bubble curve slopes, $(\partial P/\partial x)_T$ and $(\partial T/\partial x)_P$, and dew curve slopes, $(\partial P/\partial y)_T$ and $(\partial T/\partial y)_P$, have much higher multipliers on the right side of the GD equation due to the gas-phase contributions. It is thus a good idea to perform both tests in the order given.

Test 1—Combined GD Equations

As when developing the Gibbs−Konowalow laws (Rowlinson and Swinton, 1982, p 107), the fugacity form of the Gibbs−Duhem equation for the liquid phase, eq 4a, is subtracted from that of the vapor phase, eq 3, to yield

$$(y - x)\, d \ln \hat{f}_1 - (y - x)\, d \ln \hat{f}_2 = [(V^{v}_{m} - V^{l}_{m})/RT]\, dP - [(H^{v,res}_{m} - H^{l,res}_{m})/RT^2]\, dT \quad (7)$$

The perfect gas backgrounds of the gas and liquid mixtures are not at the same composition, and so their enthalpies do not cancel. Equation 7 can be rearranged in terms of the equilibrium constant $K_1 \equiv (y_1/x_1)$ and fugacity coefficients $\hat{\phi}_i \equiv (\hat{f}_i/Py_i)$ to provide

$$(K_1 - 1)x\left[\frac{dy}{y(1 - y)} + d \ln(\hat{\phi}_1/\hat{\phi}_2)\right] = [(V^{v}_{m} - V^{l}_{m})/RT]\, dP - [(H^{v,res}_{m} - H^{l,res}_{m})/RT^2]\, dT \quad (8)$$

Again, the low-pressure vapor will be assumed to be either a perfect gas mixture (PGM; $\hat{\phi}_i = 1$) or a second virial gas mixture (SVGM) where

$$\ln(\hat{\phi}_1/\hat{\phi}_2) = (P/RT)[(B_{11} - B_{22}) + (1 - 2y)\delta_{12}] \quad (9)$$

The identity of eq 8 together with a gas model provides calculation of x from measurements of (P, y) at constant T, provided a reasonable estimate of ($V_m^v - V_m^l$) can be made. Similarly for constant pressure measurements, x can be found from measurements of (T, y) at constant P, provided a reasonable estimate of ($H_m^{v,res} - H_m^{l,res}$) can be made. The reverse problem of calculation of y from x is far more difficult in practice for several nontrivial reasons; this asymmetry between the gas and liquid is created by the fact that we are measuring nonideal liquid solutions at low pressures where the vapor phase is approaching a PGM, a very special ideal solution, so that measuring (P, T, y) provides the fugacities of eq 1 whereas knowing (P, T, x) does not because at least one of the liquid-phase activity coefficients is usually much different from unity. This same feature is seen on the right side of eq 7 at constant T, where accurate knowledge of V_m^v is far more important than that of the much smaller V_m^l. Of course these differences disappear upon approaching a mixture vapor/liquid critical point but not a noncritical azeotrope.

Because a binary VLE data set cannot be both isothermal and isobaric, both the liquid-side and vapor-side forms of the Gibbs−Duhem equation contain a nonzero term involving a bubble-point or a dew-point slope. This is due to the phase rule which provides only a single datum, fixed x and y, when both temperature and pressure are set. Except at an azeotrope, the right-hand side of the GD equation should never be ignored or declared negligible without at least estimation of its magnitude. Because this assumption has been made for so long in most undergraduate texts, generations of practicing engineers believe a number of data sets to be inconsistent when they are not. An example involving activity coefficients and the liquid Gibb−Duhem equation will be given later.

Test 1—Applications to VLE Data

Isothermal Measurements (Test 1T). Using eqs 8 and 9 for a SVGM in the vapor,

$$x = y - \left\{ \frac{(\partial P/\partial y)_T (RT/P)(Z_m^v - Z_m^l)}{(RT/y(1-y)) - 2\delta_{12}P + (\partial P/\partial y)_T[(B_{11} - B_{22}) + (1-2y)\delta_{12}]} \right\} \quad (10)$$

Unlike a similar equation used by McGlashan (1979), eq 10 is exact when the vapor is a SVGM. McGlashan (1979) used a liquid-side GD equation with both right-side terms set to zero, as discussed in the previous section; that is, the excess volume of the liquid mixture was ignored. A very complete discussion of this derivation and this assumption is found in McGlashan (1979). When the vapor phase is near an ideal solution, as for many hydrocarbon mixtures, $\delta_{12} = 0$. For a PGM, eq 10 reduces to the more familiar result

$$x = y[1 - (1-y)(\partial \ln P/\partial y)_T(1 - Z_m^l)] \quad (11)$$

In most cases Z_m^l can be ignored compared to Z_m^v. The real value of the SVGM model is that the effect of the second virial coefficients can be used to find the difference between x(eq 10) and x(eq 11). When this difference is less than roughly 0.01, then major discrepancies between x(exp) and x from either eq 10 or eq 11 cannot be attributed to gas-phase imperfections. Because x has been calculated from experimental values of (P, y), disagreement of x(exp) with x(cal) by 0.05 or more is usually caused by (1) failure to measure x and/or y accurately and/or (2) failure to measure P accurately, so that $(\partial \ln P/\partial y)_T$ is not accurately found from the data. This second problem is often acute at dilution, where eq 10 as $y \to 0$ becomes (Eubank et al., 1987)

$$x = y[1 - (\partial \ln P/\partial y)_T^\infty (1 + (B_{22}P_2^\sigma/RT))] \quad (12)$$

In such a case the pressure derivative should be evaluated from a numerical forward or backward difference formula such as that of Newton (*CRC Handbook of Mathematical Tables*, 1964).

Experimental variations in T should not be a problem for modern measurements using platinum resistance thermometers easily capable of measurement to ±1 mK. However, impurities remain a frequent major error source with their error propagation often being many times the impurity fraction itself (Eubank et al., 1987).

Simple Example. We first present some simple examples that both authors and reviewers can perform in minutes with hand calculators. Later, we provide a more detailed analysis using a digital computer to study the effect of the assumed gas model.

Consider, for example, the data of Udovenko and Fatkulina (1952) for ethanol (1) + water (2) at 40 °C. They report the data at $y = 0.3160$, $x = 0.0580$, and $P = 10.61$ kPa. From this datum and neighboring data, we find that $(\partial P/\partial y)_T = 14.41$ kPa or $(\partial \ln P/\partial y)_T = 1.358$. Also, $Z_m^l = 8.25 \times 10^{-5}$, so eq 11 yields $x = 0.0225$, whereas eq 10 yields $x = 0.0236$. If the experimental values of y are correct, then $(\partial \ln P/\partial y)_T = 1.194$ or $(\partial P/\partial y)_T = 12.7$ kPa—a 13.8% difference, whereas the difference in x is of the order of 90%. Different numerical methods for evaluation of this slope provide essentially the same results; rough error analysis shows that errors of ±0.01 in x and in y plus ±1% in pressure can cause errors as high as 20% in $(\partial P/\partial y)_T$—this is likely the problem with these data.

Isobaric Measurements (Test 1P). Here the lack of mixture enthalpy data generally forces more restrictive assumptions onto the right side of eq 8. When the enthalpy of both pure liquids is set to zero at say their NBP (where the pressure $P°$ is atmospheric), the enthalpy of a liquid mixture of these two may differ from zero by the excess enthalpy due to the liquid solution being nonideal. The complete result for the SVGM is that in eq 8

$$(H_m^{v,res} - H_m^{l,res}) = -H^E + P°[(B_{11} - B_{22}) - T(B'_{11} - B'_{22})]\Delta + P°[\delta_{12} - T\delta'_{12}]y(1-y) + \langle C^*_{P1}\rangle(T - T_1^\sigma)x + \langle C^*_{P2}\rangle(T - T_2^\sigma)(1-x) + \lambda_1 x + \lambda_2(1-x) \quad (13)$$

and

$$[\partial \ln(\hat\phi_1/\hat\phi_2)/\partial y]_P = (P°/R)\left[\frac{d(B_{11}/T)}{dT} - \frac{d(B_{22}/T)}{dT} + (1-2y)\frac{d(\delta_{12}/T)}{dT}\right]\left(\frac{\partial T}{\partial y}\right)_P - (2\delta_{12}P°/RT)\left[1 - (y/T)\left(\frac{\partial T}{\partial y}\right)_P\right] \quad (14)$$

where λ_i is the enthalpy of vaporization of pure component i, the prime superscript denotes a total derivative with respect to temperature, $P°$ is the standard-state pressure of 1 bar (100 kPa), $\Delta \equiv y - x$, and $\langle C^*_{Pi}\rangle$ is the average perfect-gas isobaric heat capacity of pure component i. Numerical tests with very nonideal liquid mixtures and with the highest values of δ_{12}, such as from acetonitrile + acetaldehyde and methanol + benzene, have shown that the second, fourth, and fifth terms on the RHS of eq 13

are negligible, as are all the terms on the RHS of eq 14 except for $[-(2\delta_{12}P^o/RT)]$ alone. Equation 8 then simplifies to

$$x \cong \{\lambda_1 x + \lambda_2(1-x) + P°y(1-y)[\delta_{12} - T\delta'_{12}] - H^E\} \times [RTy^{-1}(1-y)^{-1} - 2\delta_{12}P°]^{-1}(\partial \ln T/\partial y)_P + y \quad (15)$$

Now we move on to the PGM assumption for the vapor and also ignore the liquid excess enthalpy in eq 15 in comparison to the higher enthalpies of vaporization. Excess enthalpies are usually <1 kJ/mol, whereas enthalpies of vaporization are typically of the order of (25−35) kJ/mol. A particularly simple and useful equation results:

$$x = y[1 + (1-y)(x\lambda_1 + (1-x)\lambda_2)(\partial T/\partial y)_P/RT^2] \quad (16)$$

While eq 16 is by no means exact, it has been found, like eq 11, to provide values of x usually within the experimental error of x itself when the (T, x, y) measurements are consistent with GD. Equations 15 and 16 have not been solved explicitly for x, as they can be applied most easily by using x(exp) on the right side to calculate x(cal) on the left side for comparison to x(exp). Equation 16 is sufficiently simple that it can be apply to the approximately 50% of existing isobaric data where the pure enthalpies of vaporization are known independently. Otherwise, these enthalpies of vaporization can be estimated, usually to about ±2%, from the NBP temperature and critical properties by methods reviewed in Reid et al. (1986). When experimental excess enthalpy measurements are available, the mixture second virial coefficients of eq 15 can be estimated by the method of Tsonopoulos (1974); then x(eq 15) can be compared to x(eq 16) and to x(exp) to see the effect of the gas model and whether the data are consistent.

Simple Example. An example is the recent measurements of Loras et al. (1999) for 3-methylpentane (1) + diisopropyl ether (2) at 101.3 kPa; a total of 22 data points were taken for different values of x with temperatures ranging monotonically from 336.3 K (x = 1) to 341.4 K (x = 0). The pure-component enthalpies of vaporization are λ_1 = 28.1 kJ/mol and λ_2 = 29.1 kJ/mol (Majer and Svoboda, 1985). For the datum y = 0.089, x = 0.069, and T = 340.6 K, neighboring data provide $(\partial T/\partial y)_P = -7.42$ K, so eq 16 yields x = 0.071, in close agreement with experiment. Experimental excess enthalpies for the liquid were not found.

Test 1—New Graphical Method

Most experimentalists are rightfully reluctant to use models in conjunction with their data—even numerical differentiation formulas such as Newton forward, Newton backward, and Stirling central difference for the derivatives appearing in eqs 10, 11, 15, and 16. We present here a new graphical method for test 1 that can be used regardless of the assumed gas model. Nevertheless, for simplicity, we first illustrate the graphical method for a PGM. Let $\Delta \equiv y - x$; $P^* \equiv \ln(P/P_2^o)$; and $T^* \equiv -\ln(T/T_2^o)$. For isothermal data, plot P^* versus y, as shown in Figure 1. Note that P^* is zero at y = 0, whereas, at y = 1, $P^* = \ln(P_1^o/P_2^o)$ and azeotropes must appear as extrema similar to P versus y. Further, $(\partial P^*/\partial y)_T = (\partial \ln P/\partial y)_T$, so that eq 11 with $1 \gg Z_m^l$ becomes

$$\Delta° = y(1-y)(\partial P^*/\partial y)_T \quad (17)$$

but $y(\partial P^*/\partial y)_T = P^* - I$, where I is the intercept of the tangent line drawn to the data at (y, P^*), as shown in Figure 1. Thus, $\Delta^o = (1-y)(P^* - I)$, the area of the rectangle of Figure 1. This area assumes the sign of $(P^* - I)$, which can be positive or negative. The superscript ° above Δ denotes the PGM assumption.

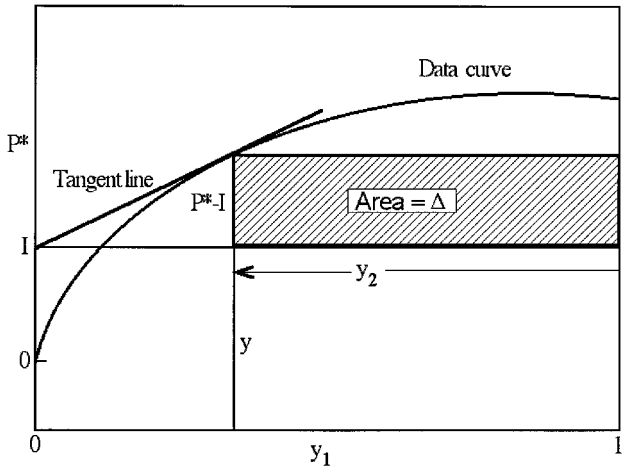

Figure 1. New graphical procedure for checking the consistency of VLE data via test 1. Here $P^* \equiv \ln(P/P_2^o)$ and I is the intercept on the ordinate of the tangent line drawn from the known value of y. The area shown equals $y - x$.

When using eq 10 for the SVGM, the procedure is similar using the same graph, except

$$\Delta = (Z_m^v - Z_m^1)(\text{area})\left[1 - \frac{2\delta_{12}y(1-y)P}{RT} + [B_{11} - B_{22} + (1-2y)\delta_{12}](P/RT)(\text{area})\right]^{-1} \quad (18)$$

where the area (or Δ°) is the same as that of Figure 1. Equation 18 should yield Δ to ±0.001 for pressures below 2 bar, subject, of course, to errors in the separate quantities on the right side of the equation. This equation reduces to eq 17 for a PGM with $1 \gg Z_m^l$.

For isobaric data with eq 16, the procedure is again similar, except T^* is graphed against y. Because

$$\Delta° = -(x\lambda_1 + (1-x)\lambda_2)y(1-y)(\partial T/\partial y)_P/RT^2 \quad (19)$$

the area corresponding to Figure 1 must be multiplied by $(x\lambda_1 + (1-x)\lambda_2)/RT$ to provide Δ°. As an alternate procedure, $T^{**} \equiv (T_2^\sigma/T)$ can be graphed against y with the area corresponding to Figure 1 multiplied by $(x\lambda_1 + (1-x)\lambda_2)/RT_2^\sigma$ to provide Δ°. In any case, the x in the multiplier is taken from experiment, as described following eq 16. For the SVGM, eq 15 leads to

$$\Delta = \{[H^E - P°y(1-y)(\delta_{12} - T\delta'_{12})](\partial \ln T/\partial y)_P + RTy^{-1}(1-y)^{-1}\Delta°\}[RTy^{-1}(1-y)^{-1} - 2\delta_{12}P°]^{-1} \quad (20)$$

Lamonte (1999) has selected several isothermal and several isobaric data sets from Ohe (1989) for use with these graphical procedures. These data sets are (a) chloroform (1) + ethanol (2) at 45 °C, (b) carbon tetrachloride (1) + acetonitrile (2) at 45 °C, (c) bromopentafluoride (1) + bromotrifluoride (2) 74.9 °C, (d) methyl acetate (1) + methanol (2) at 30 °C, (e) chloroform (1) + 2,3-dimethylbutane (2) at 1.10325 bar, (f) chloroform (1) + benzene (2) at 1.10325 bar, (g) ethanol (1) + aniline (2) at 1.10325 bar, and (h) methanol (1) + carbon tetrachloride (2) at 1.10325 bar.

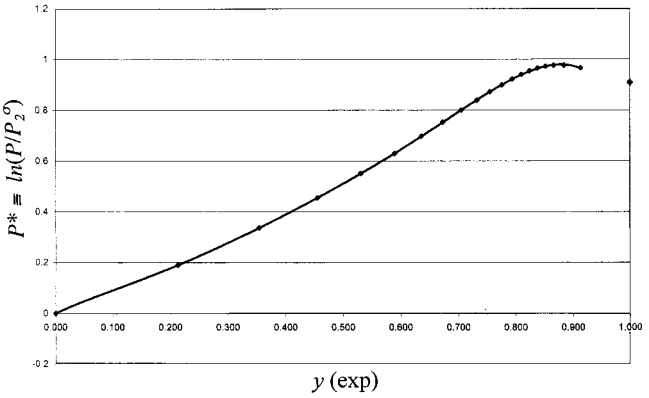

Figure 2. New graphical procedure of Figure 1 applied to chloroform (1) + ethanol (2) at 45 °C from Ohe (1989). $P^* \equiv \ln(P/P_2^\sigma)$ is plotted versus y. The line fitted to the separate data points is $P^* = (-17.048)y^6 + (39.738)y^5 - (35.949)y^4 + (15.906)y^3 - (2.977)y^2 + (1.0784)y - (0.0004)$.

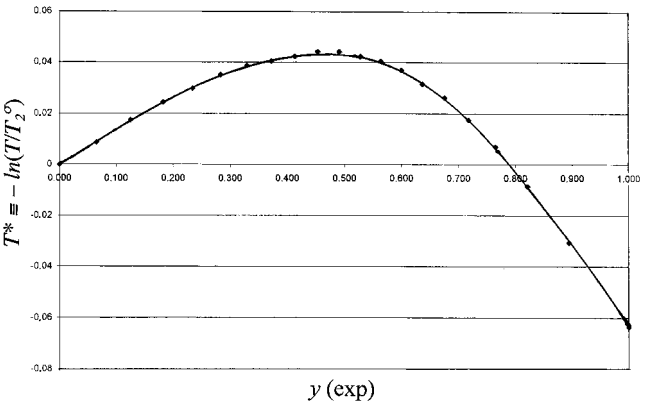

Figure 3. New graphical procedure of Figure 1 applied to chloroform (1) + 2,3-dimethylbutane (2) at 101.3 kPa from Ohe (1989). $T^* \equiv -\ln(T/T_2^\sigma)$ is plotted versus y.

Generally, good agreement was found between the calculated and experimental values of x; here *good* agreement is when the difference is no more than 0.01. One seeks agreement to 0.001, but this is not realistic considering the sensitivity to dew and bubble curve slopes discussed at the end of the next section. As an example of this agreement, Figure 2 is P^* versus y for set (a), where, at $y = 0.794$, x (exp) = 0.600, $P = 57.95$ kPa, $P_1^\sigma = 57.36$, $P_2^\sigma = 23.05$, and x(graph) = 0.606 without virial coefficient correction. Conversely, Figure 3 is T^* versus y for set (e), where, at $y = 0.765$, x(exp) = 0.850, $T = 57.5$ °C, $T_1^\sigma = 61.7$ °C, $T_2^\sigma = 57.9$ °C, $\lambda_1 = 29.2$ kJ/mol, $\lambda_2 = 27.3$ kJ/mol, and x(graph) = 1.24!, without virial coefficient correction. However, corrections with the SVGM, as detailed in the next section, and an estimate of the excess enthalpy for the liquid are too small to change this result.

Test 1—Effect of the Assumed Gas Model

Alvarado (1999) has performed a study of the effect of the assumed gas model, whether PGM or SVGM, on the values of x calculated under test 1 for both the isothermal and the isobaric cases. Alvarado used the Tsonopoulos correlation (1974) for B_{ii} and B_{ij} but also found no significant changes in his results with the somewhat simpler correlations found in Smith et al. (1996). Further, Alvarado took critical constants, acentric factors, and so forth from Reid et al. (1986). Alvarado's results are now summarized.

Isothermal Measurements (Test 1T). Six literature systems were studied: (a) acetone (1) + methanol (2) at 373.15 K from Griswold and Wong (1952), (b) 2-butanone (1) + *n*-heptane (2) at 318.15 K from Takeo et al. (1979), (c) *n*-heptane (1) + 2-methyl-1-butanol (2) at 368.15 K from Wolfova et al. (1991), (d) ethanol (1) + water (2) at 313.15 K from Udovenko and Fatkulina (1952), (e) methanol (1) + methyl methacrylate (2) at 323.15 K from Ishikawa and Lu (1979), and (f) methanol (1) + *tert*-amyl methyl ether (2) at 333.15 K from Toghiani et al. (1996). Here the difference between the PGM (eq 11) and SVGM (eq 10) can be significant especially when δ_{12} differs significantly from zero. Comparison of the first two terms in the denominator of the last quantity of eq 10 shows that when $y = 0.5$, so that the dominant term $[y(1 - y)]^{-1}$ is 4, the term $[2\delta_{12}P/RT]$ is 1% of 4 or 0.04 when $\delta_{12} = \pm 540$ cm^3/mol for $P = 1$ bar and $T = 325$ K. Considering that absolute values of δ_{12} can range from zero to as much as 10 times this value, significant differences between PGM and SVGM results can occur in the middle of the P versus y diagram but not approaching either end, as $[y(1 - y)]^{-1}$ is divergent.

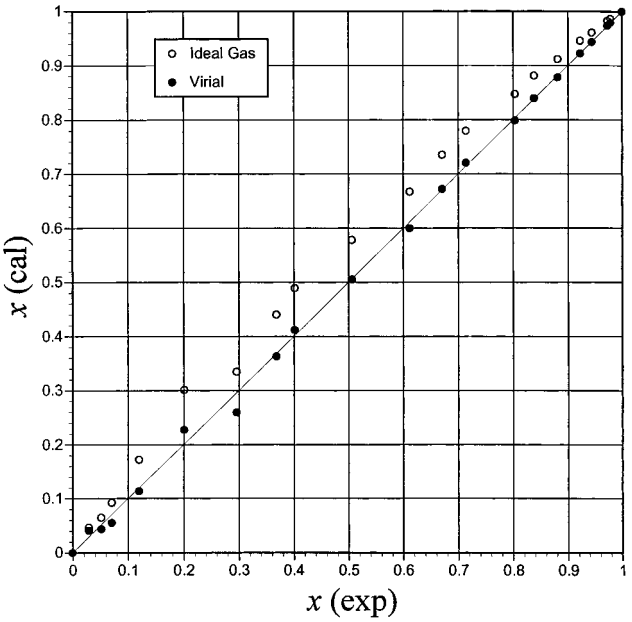

Figure 4. New graphical procedure of Figure 1 applied to methanol (1) + methyl methacrylate (2) at 323.15 K from Ishikawa and Lu (1979). Here values of x are calculated from eq 11 assuming the vapor to be a perfect gas mixture (○) or from eq 10 assuming the vapor to be a SVGM (●). The calculated values of x are graphed against the experimental values of x. The correction of the vapor with a SVGM is seen to significantly improve the agreement.

The results of Alvarado (1999) show significant differences for all six systems except (b), where the differences in the calculated x are less than 0.02 but the SVGM does improve the agreement between x(exp) and x(cal) to be less than 0.01 for 18 data points. In all cases but (d), x(cal) agrees significantly better with x(exp) when the SVGM is used; a good example is case (e) shown by Figure 4. Figure 5 shows that the data of case (d) suffer problems for y in the range 0.1−0.6 that cannot be reconciled by either gas model.

Isobaric Measurements (Test 1P). Alvarado studied 10 isobaric VLE data sets: (a) 1-propanol (1) + water (2) at 26.7 and 80.0 kPa from Smirnova (1959), (b) 1-propanol (1) + *n*-octane (2) at 101.3 kPa from Hiaki et al. (1995), (c) 2-propanol (1) + acetonitrile (2), 2-propanol (1) + 1-chlorobutane (2), and 1-chlorobutane (1) + acetonitrile (2) at 101.3 kPa from Tu and Ou (1998), (d) acetone (1) + benzene (2) at 101.3 kPa from Canjar et al. (1956), (e) acetone (1) + chloroform (2) at 101.3 kPa from Reinders and de Minjer

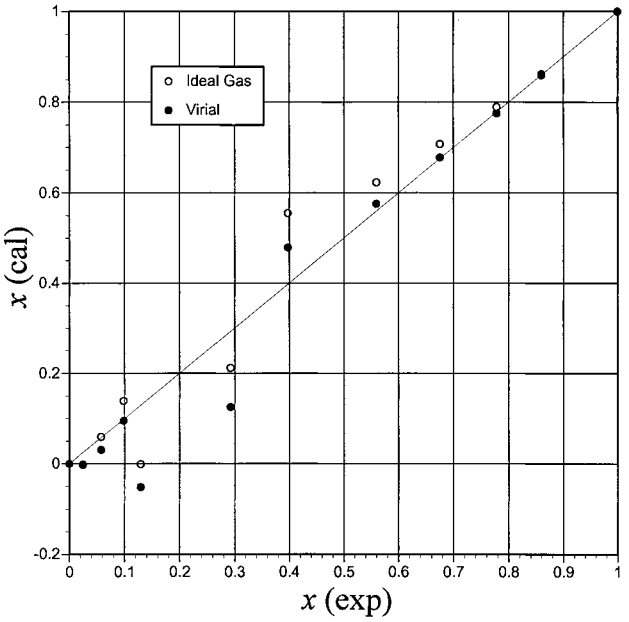

Figure 5. New graphical procedure of Figure 1 applied to ethanol (1) + water (2) at 313.15 K from Udovenko and Fatkulina (1952). Here values of x are calculated from eq 11 assuming the vapor to be a perfect gas mixture (○) or from eq 10 assuming the vapor to be a SVGM (●). The calculated values of x are graphed against the experimental values of x. Serious problems are seen to exist with these data although the experimental P versus y curve is smooth.

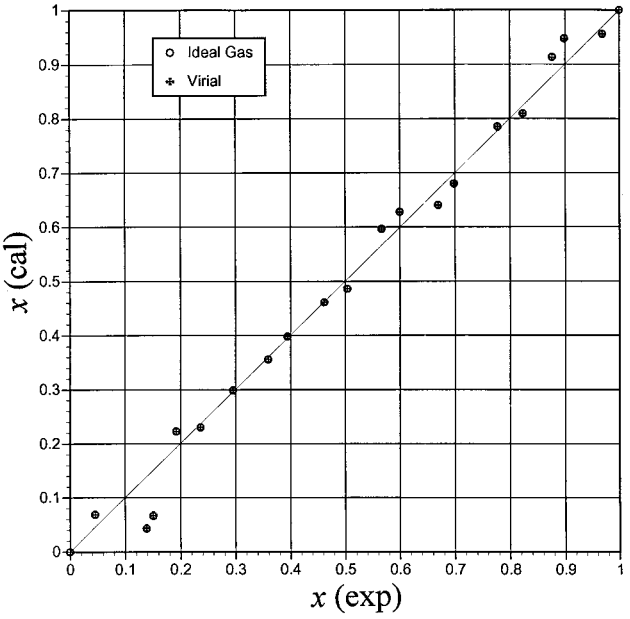

Figure 6. New graphical procedure of Figure 1 applied to 2-propanol (1) + 1-chlorobutane (2) at 101.3 kPa of Tu and Ou (1998). Here values of x are calculated from eq 16 assuming the vapor to be a perfect gas mixture (○) or from eq 15 assuming the vapor to be a SVGM (●). The calculated values of x are graphed against the experimental values of x. The agreement is generally good excepting two outliers near $x = 0.15$.

(1940), and (f) methanol (1) + benzene (2) at 101.3 kPa from Fritzweiler and Dietrich (1933) and also later by Kurihara et al. (1998). He found the difference between x(eq 15) and x(eq 16) to be <0.01 although >0.001 in most cases. Most of these data sets provide good agreement between x(calc) and x(exp), as seen in Figure 6 for 2-propanol (1) + 1-chlorobutane (2) at 101.3 kPa of Tu and Ou

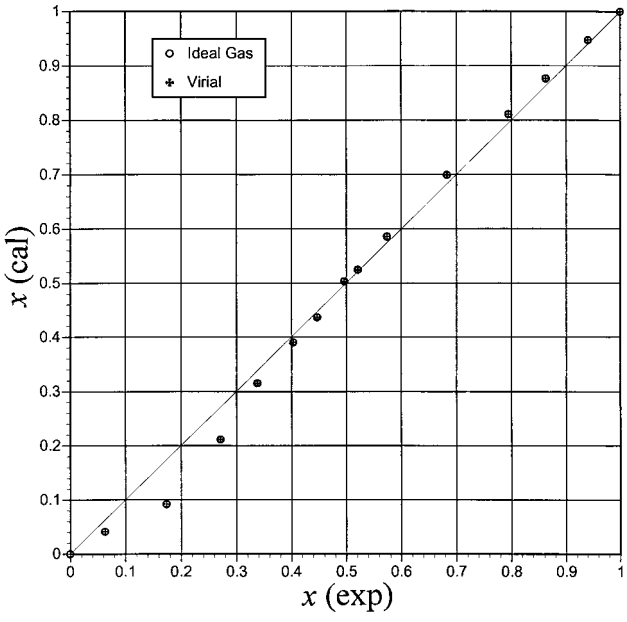

Figure 7. New graphical procedure of Figure 1 applied to acetone (1) + benzene (2) data at 101.3 kPa from Canjar et al. (1956). Here values of x are calculated from eq 16 assuming the vapor to be a perfect gas mixture (○) or from eq 15 assuming the vapor to be a SVGM (●). The calculated values of x are graphed against the experimental values of x. A small systematic bias is seen in the difference between the calculated and experimental values of x as x increases.

(1998). Of the three systems measured by these investigators, case (c), this system shows the highest scatter about x(calc) in the plot against x(exp). Alvarado estimated $(\partial T/\partial y)_P$ from a cubic spline fit; he also provided a graph of $(\partial T/\partial y)_P$ versus y for each system. However, in some cases there is scatter on these graphs that carries over to the final results of x(calc) versus x(exp). Once the $(\partial T/\partial y)_P$ versus y graph is smoothed for use in eq 15 or 16, then most of the scatter is eliminated from the final results.

It is thus one of the pitfalls of test 1 that one cannot take $(\partial T/\partial y)_P$ or $(\partial P/\partial y)_T$ by differencing the experimental data from one datum to the next. Rather one must try to smooth the data so that the derivatives appearing in eq 15 or 10 are themselves smooth. Otherwise the final graph of x(calc) versus x(exp) will show high scatter but no systematic bias for x(calc) − x(exp). For example, the acetone (1) + benzene (2) data at 101.3 kPa from Canjar et al. (1956) show a small bias, as seen in Figure 7, while our curve of $(\partial T/\partial y)_P$ is well smoothed. This is also true of our curve of $(\partial P/\partial y)_T$ for the data in Figure 5.

Test 2—Activity Coefficients

Equation 6 provides for calculation of the activity coefficients from (P, T, y, x) data, hopefully after passing test 1. The activity coefficients are particularly sensitive to the vapor model, so the SVGM should be used here even though it was found earlier that there was no difference between eqs 10 and 11 for isothermal data or between eqs 15 and 16 for isobaric data. Equation 4b should be written with x as the independent variable, so that for isothermal data

$$x(\partial \ln \gamma_1/\partial x)_T + (1 - x)(\partial \ln \gamma_2/\partial x)_T = (V_1^E/RT)(\partial P/\partial x)_T \quad (21)$$

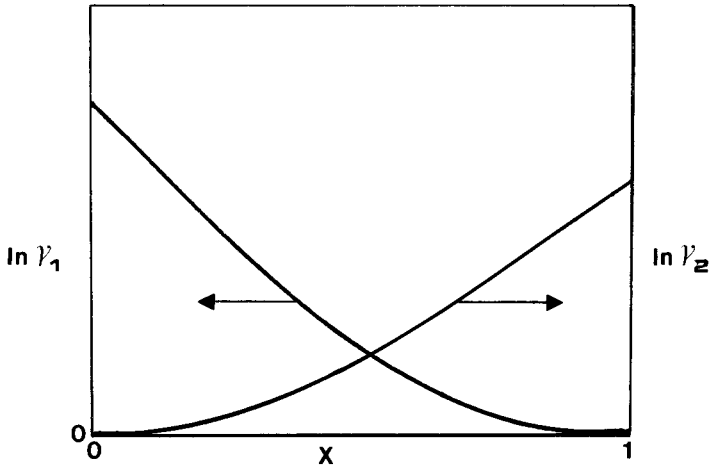

Figure 8. Common graph of the natural logarithm of the activity coefficient of component 1 and also component 2 versus the liquid-phase mole fraction x.

and for isobaric data

$$x(\partial \ln \gamma_1/\partial x)_P + (1 - x)(\partial \ln \gamma_2/\partial x)_P = -(H_1^E/RT^2)(\partial T/\partial x)_P \quad (22)$$

The resultant values of the activity coefficients, whether from isothermal or isobaric data, should further be tested (test 2) with these well-known GD forms for only the liquid phase. While test 2 and test 1 are theoretically equivalent, as discussed earlier, a number of data sets can be shown to obey eq 10 (or eq 15) but fail eq 21 (or eq 22). The reason for this paradox is that test 1 is a vapor-GD minus liquid-GD test that drowns out the RHS of the liquid-GD equation; V^E and H^E for the liquid are too small to be of importance in eqs 10 and 15, respectively, but they are very important in eqs 21 and 22, respectively. These equations do not use the vapor-GD equation, which is automatically satisfied by the assumption of a vapor model, and so test 2 is sensitive to deviations from an ideal liquid solution.

While these equations are among the most important in solution thermodynamics, evaluation of the right side is often difficult due to uncertainties both in the excess function and in the slope term. However, if the tests of the previous sections have been successful—that is, if (x, y, P) are consistent by eq 10 (or eq 11 at low pressures) for isothermal data—then the slope in eq 10 is correct and one need only be concerned about the excess function when examining the familiar graphs of ($\ln \gamma_i$) versus x as illustrated by Figure 8. There it is obvious from eqs 21 and 22 that as $x_i \rightarrow 1$, both $y_i \rightarrow 1$ and $(\partial \ln \gamma_i/\partial x_i) \rightarrow 0$ (solvent limits).

A general order-of-magnitude analysis shows that, because V^E is seldom >1 cm^3/mol and H^E is seldom >1 kJ/mol in absolute value (Rowlinson and Swinton, 1982, Chapter 5), the quantities (V^E/RT) and (H^E/RT^2) are seldom $>4 \times 10^{-5}$ bar^{-1} and 1.3×10^{-3} K^{-1}, respectively. Similarly, it is unusual for the absolute values of the bubble-point curve slopes $(\partial P/\partial x)_T$ and $(\partial T/\partial x)_P$ to exceed 1 bar and 100 K, respectively, for low-pressure VLE measurements. Thus, the right hand sides of eqs 21 and 22 seldom exceed 4×10^{-5} and 0.13, respectively. To approximate the terms on the left hand sides of eqs 21 and 22, imagine that γ_1 followed Porter's symmetric model

$$\ln \gamma_1 = Ax_2^2 \quad (23)$$

where $\ln \gamma_1^\infty = A$ and γ_1^∞ is generally greater than 1.1, so $A > 0.0953$. The first term on the LHS of either eq 21 or eq 22 is $-2Ax_1x_2$, which reaches its maximum absolute value of 0.0477 for the equimolar liquid but drops to $^4/_9$ of that value or 0.0172 when x is 0.1 or 0.9. If the second term on the LHS of either eq 21 or eq 22 were zero at $x = 0.1$, then we see that the RHS of eq 21 is not likely to compensate whereas the RHS of eq 22 may compensate, remembering that the maximum value of 0.13 above likely is near equimolar and will drop considerably at $x = 0.1$. The result here for test 2 is that isothermal data at any x showing the same sign for the slopes $(\partial \ln \gamma_1/\partial x_1)_T$ and $(\partial \ln \gamma_2/\partial x_1)_T$ are very unlikely to obey eq 21, as the RHS is far too small to compensate. For isobaric data, compensation from the RHS of eq 22 is a possibility to be checked by first examination of the sign of H^E; nevertheless, the occurrence of the same signs for the two terms on the LHS of either eq 21 or eq 22 should be a warning signal for careful testing of the data. This occurrence usually arises on approaching dilution with the activity coefficient of the solvent dropping below unity, dropping through a minimum, and then returning to unity with zero slope, as shown with some exaggeration in Figure 9. Even for isobaric data, such behavior is usually not real but rather the result of one or both of the following two reasons: (a) the virial coefficients

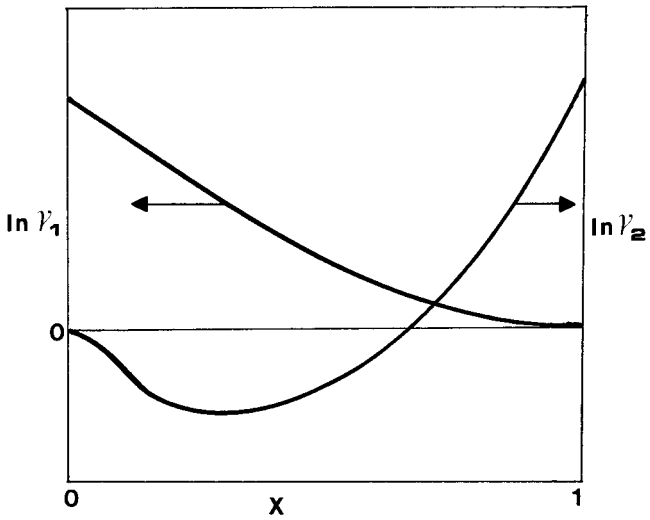

Figure 9. Figure 8, but showing qualitatively data where the ln γ_2 upon approaching the pure 2 endpoint falls below zero (γ_2 falls below unity). The inflection shown in the curve of ln γ_2 on the right side of the diagram does not violate the GD eq and is forecast by the two-constant Margules equation (see Smith et al., 1996, p 376).

Table 1. Correction of Data of Martinez-Soria et al. (1999) for *tert*-Butyl Alcohol (1) + Toluene (2) at 101.3 kPa via Graphical Method of Test 1 at Low Values of *x*

T/K	T*	x(exp)	x(cal)	y(exp)	γ_1(exp)	γ_1(cal)	γ_2(exp)	γ_2(cal)
383.8	0	0	0	0		1.963	1	1
379.3	0.01179	0.0236	0.0330	0.1504	2.814	2.012	0.983	0.993
375.7	0.02133	0.0464	0.0599	0.2440	2.602	2.016	0.992	1.006
371.4	0.03284	0.0821	0.1014	0.3621	2.512	2.034	0.986	1.007
370.4	0.03554	0.0878	0.1163	0.3769	2.528	1.908	0.998	1.030
368.6	0.04041	0.1090	0.1390	0.4156	2.386	1.871	1.011	1.046
366.2	0.04694	0.1529	0.1891	0.4842	2.151	1.739	1.010	1.055
363.5	0.05434	0.2083	0.2561	0.5518	1.978	1.609	1.021	1.087
361.7	0.05931	0.2503	0.2932	0.5807	1.847	1.577	1.067	1.132
360.4	0.06291	0.3140	0.3445	0.6189	1.645	1.499	1.105	1.156
359.5	0.06541	0.3846	0.4298	0.6547	1.468	1.314	1.149	1.240
358.3	0.06875	0.4802	0.5138	0.6928	1.300	1.215	1.258	1.345
357.8	0.07015	0.5213	0.5489	0.7072	1.245	1.182	1.323	1.404
357.2	0.07183	0.5787	0.6100	0.7281	1.181	1.120	1.423	1.537
357.0	0.07239	0.6108	0.6504	0.7464	1.155	1.085	1.447	1.611
356.8	0.07295	0.6398	0.6821	0.7620	1.134	1.064	1.477	1.673
356.5	0.07379	0.6891	0.7155	0.7828	1.094	1.054	1.577	1.723
356.1	0.07491	0.7397	0.7629	0.8124	1.074	1.041	1.649	1.810
355.7	0.07603	0.8083	0.8305	0.8509	1.045	1.017	1.803	2.039
355.6	0.07632	0.8414	0.8593	0.8703	1.030	1.009	1.902	2.144
355.5	0.07660	0.9005	0.9026	0.9082	1.008	1.005	2.154	2.200
355.5	0.07660	0.9178	0.9160	0.9200	1.002	1.004	2.272	2.223
355.4	0.07688	0.9343	0.9362	0.9362	1.006	1.004	2.275	2.343
355.5	0.07660	0.9578	0.9593	0.9565	0.998	0.997	2.407	2.496
355.6	0.07632	0.9719	0.9736	0.9712	0.995	0.993	2.386	2.540
355.7	0.07603	1	1	1	1	1		2.698

have not been used in the equilibrium equation (eq 6) and/or (b) test 1 via eq 10 or 15 is not obeyed by the data, causing an inconsistency between the measured x and y as used in eq 6. The first reason is easily understood from eq 6 for ln γ_1: as x approaches unity, the δ_{12} term is effectively eliminated while the B_{11} term is positive, as both B_{11} and $(P - P_1^\sigma)$ are negative. The reverse is true for the heavy solvent, as pictured in Figure 9, so the second reason is more likely behind the problem.

An example among many is the recent isobaric data of Martinez-Soria et al. (1999), who have corrected their data with virial coefficients but, like most experimentalists, have not used test 1. Table 1 shows that when our new graphical method is used to calculate x consistent with the experimental values of y, significant differences are found with x(exp) for values of x extending to near 0.8. Use of our x(cal) in eq 6 results in values of γ_2 for toluene, the solvent, that no longer dip below unity at dilution of the solute, *tert*-butyl alcohol. Values of γ_1 are also lowered significantly for low values of x. Our infinite dilution activity coefficients in Table 1 were calculated from combination of eqs 6, 8, and 9, which provide

$$\gamma_1^\infty = (P_2^\sigma/P_1^\sigma)[1 + (\partial T/\partial y)_p^\infty(\mathrm{d}\ln P_2^\sigma/\mathrm{d}T)]^{-1} \exp\{[(B_{11} - \langle V_1^L\rangle)(P_2^\sigma - P_1^\sigma) + \delta_{12}P_2^\sigma]/RT_2^\sigma\} \quad (24)$$

for γ_1^∞, and a similar equation for γ_2^∞ results when the subscripts 1 and 2 are interchanged. All of the other calculated activity coefficients in Table 1 are the result of using the same virial coefficient corrections and pure-component vapor pressures as used by Martinez-Soria et al. (1999), so that

$$\gamma_i(\mathrm{cal}) = \gamma_i(\mathrm{exp})\cdot x_i(\mathrm{exp})/x_i(\mathrm{cal}) \quad (25)$$

It is easily seen from Table 1 that making x consistent with the (T, y) measurements via test 1 has other benefits besides removing the solvent activity coefficient problem of Figure 9. The solute activity coefficients are strongly affected and now brought into line with the infinite dilution values of eq 24. The calculated activity coefficients of Table 1 agree with test 2, allowing for experimental scatter which is not removed when test 1 is used to make x consistent with the (T, y) measurements. That is, application of test 1 does not result in a data smoothing procedure.

Experimentalists who feel that their measured values of x are superior to their measured y can adjust y instead by using eq 10 or 15 or the graphical method after some trial/error. Then values of y(cal) can be checked against y(exp) to see if y(cal) falls within the experimental error bands.

Conclusions

The use of GD equations as applied to binary VLE has been demonstrated. The double GD form of vapor minus liquid is especially advantageous because the vapor phase is inherently simpler and thus the basic consistency of (P, x, y) data at constant T or of (T, x, y) data at constant P can be checked without consideration of liquid-phase activity coefficients. Later, the liquid GD equation can be used with the activity coefficients in a conventional test. While the two tests are not independent in theory, they become so in application due to large differences in the magnitude of the terms involved. There are good reasons to apply first the double GD equation. Integral tests have not been considered because, while useful when all the RHS terms are included, they form necessary but not sufficient conditions—that is, the process of integration over x can cancel out errors that are apparent in the differential tests considered here.

Temperature and pressure *can be measured easily* to ±1 mK and ±0.02%, respectively, but such high accuracy is seldom attained in VLE experiments. The only weakness of test 1 is in the evaluation of the pressure and temperature derivatives with respect to y. Better measurements of temperature and pressures in future VLE experiments will allow test 1 to better check the internal consistency of the less accurate phase compositions.

Notation

A = single constant in Porter's symmetric model (also known as single-constant Margules)

B_{ii} = second virial coefficient of pure component i
B_{ij} = cross second virial coefficient of components i and j in a mixture
B_m = mixture second virial coefficient
$C_{p,i}^*$ = perfect-gas-state heat capacity of pure component i
$\hat{f}_i$ = fugacity of component i in a mixture
G = Gibbs energy
g = dimensionless Gibbs energy (G/RT)
H = specific enthalpy
K_i = equilibrium constant (y_i/x_i)
LHS = left-hand-side
P = pressure
PC = dimensionless Poynting correction
R = universal gas constant
RHS = right-hand-side
T = temperature, absolute
V = specific volume
x = liquid-phase mole fraction (composition)
y = vapor-phase mole fraction (composition)
Z = compressibility factor (PV/RT)

Greek Symbols

γ_i = activity coefficient of component i in the liquid solution
Δ = the difference ($y - x$)
δ_{12} = mixture second virial coefficient parameter showing deviation from ideal solution in the vapor, $2B_{ij} - B_{ii} - B_{jj}$
λ_i = heat of vaporization of pure component i
ϕ_i = fugacity coefficient of component i

Subscripts

i = component i
m = mixture

Superscripts

E = excess property
L, l = liquid phase
° = property at standard pressure of 1 bar
res = residual property, real property less perfect gas property at same (P, T, x)
v = vapor phase
σ = property at saturation
∞ = mixture property at infinite dilution of subscript i
* = perfect gas property
` = prime indicates temperature derivative
^ = carat indicates a property in the mixture

Literature Cited

Abbott, M. M.; Prausnitz, J. M. Modeling the Excess Gibbs Energy. In *Models for Thermodynamic and Phase Equilibria Calculations*; Sandler, S. I., Ed.; Marcel Dekker: New York, 1994; Chapter 1.

Alvarado, J. J. *Studies on Phase Equilibrium Calculations*; Rpt. from Inst. Tecn. de Celaya, Depto. de Ingenieria Quimica, Celaya, Gto., Mexico, June 11, 1999.

Canjar, L. N.; Horni, E. C.; Rothfus, R. R. Vapor-Liquid Equilibrium in Acetone-Benzene-Ethylene Dichloride System. *Ind. Eng. Chem.* **1956**, *48*, 427.

Dymond, J. H.; Smith, E. B. *The Virial Coefficient of Pure Gases and Mixtures*; Oxford University Press: Oxford, 1980.

Eubank, P. T. A Review of Experimental Techniques for Vapor-Liquid Equilibria at High Pressures. In *Phase Equilibria and Fluid Properties in the Chemical Industry (Proceedings, Part II)*; Knapp, H., Ed.; DECHEMA: Frankfurt/Main, 1980; pp 675−687.

Eubank, P. T.; Kim, E. S.; Holste, J. C.; Hall, K. R. Effect of Impurities upon Pure Component Thermophysical Properties. *Ind. Eng. Chem. Res.* **1987**, *26*, 2020−2024.

Fritzweiler, R.; Dietrich, K. R. *Beih. Angew. Chem. U. Fabr. Heft* **1933**, 4.

Gmehling, J.; Onken, U. *Vapor-Liquid Equilibrium Data Collection*; Chemistry Data Series; DECHEMA: Frankfurt/Main, Germany, 1990.

Griswold, J.; Wong, S. Y. *Chem. Eng. Prog. Symp. Ser. 3* **1952**, *48*, 18.

Hala, E.; Pick, J.; Fried, V.; Vilim, O. *Vapour-Liquid Equilibrium*, 2nd ed.; Pergamon Press: Oxford, 1967.

Hala, E.; Wichterle, I.; Polak, J.; Boublik, T. *Vapour-Liquid Equilibrium Data at Normal Pressures*; Pergamon Press: New York, 1968.

Handbook of Mathematical Tables, 2nd ed.; Chemical Rubber Co.: Cleveland, OH, 1964; p 516.

Hiaki, T.; Takahashi, K.; Tsuji, T.; Hongo, M.; Kojima, K. Vapor-Liquid Equilibria of 1-Propanol or 2-Propanol with Octane at 101.3 kPa. *J. Chem. Eng. Data* **1995**, *40*, 274−276.

Ishikawa, T.; Lu, B. C. Y. Vapor-Liquid Equilibria of the Methanol-Methyl Methacrylate System at 313.15, 323.15 and 333.15 K. *Fluid Phase Equilib.* **1979**, *3*, 23−34.

Kurihara, K.; Hori, H.; Kojima, K. Vapor-Liquid Equilibrium Data for Acetone + Methanol + Benzene, Chloroform + Methanol + Benzene, & Constituent Binary Systems at 101.3 kPa. *J. Chem. Eng. Data* **1998**, *43*, 264−268.

Lamonte, B. G. *Dr. Eubank's New Graphical Method*; Rpt. from CHEN 633, Department of Chemical Eng., Texas A&M University, June 12, 1999.

Loras, S.; Aucejo, A.; Muñoz, R.; Wisniak, J. Isobaric Vapor-Liquid Equilibrium in the Systems 3-Methylpentane + Ethyl 1,1-Dimethylethyl Ether, + Diisopropyl Ether, and + Tetrahydrofuran. *J. Chem. Eng. Data* **1999**, *44*, 583−587.

Majer, V.; Svoboda, V. *Enthalpies of Vaporization of Organic Compounds*; IUPAC Chem. Data Series 32; Blackwell Sci. Pub.: Oxford, 1985.

Malanowski, S. Experimental Techniques in Vapour-Liquid Equilibrium (VLE), Low Pressure. In *Phase Equilibria and Fluid Properties in the Chemical Industry (Proceedings, Part II)*; Knapp, H., Ed.; DECHEMA: Frankfurt/Main, 1980; pp 661−674.

Marsh, K. N. Thermodynamic Excess Functions of Binary Liquid Mixtures. *Chemical Thermodynamics (Specialist Periodical Reports, Vol. 2)*; The Chemical Society: London, 1978; Chapter 1.

Martìnez-Soria, V.; Peña, M. P.; Monton, J. B. Vapor-Liquid Equilibrium for the Binary Systems *tert*-Butyl Alcohol + Toluene, + Isooctane, and + Methylcyclohexane at 101.3 kPa. *J. Chem. Eng. Data* **1999**, *44*, 148−151.

McGlashan, M. L. *Chemical Thermodynamics*; Academic Press: London, 1979; p 248.

Ohe, S. *Vapor-Liquid Equilibrium Data*; Elsevier: New York, 1989.

Raal, J. D. Characterization of Differential Ebulliometers for Measuring Activity Coefficients. *AIChE J.* **2000**, *46*, 210−220.

Reid, R. C.; Prausnitz, J. M.; Poling, B. E. *The Properties of Gases & Liquids*, 4th ed.; McGraw-Hill: New York, 1987; pp 225−229.

Reinders, W.; de Minjer, C. H. *Recl. Trav. Chim. Pays-Bas* **1940**, *59*, 369.

Rowlinson, J. S.; Swinton, F. L. *Liquids & Liquid Mixtures*, 3rd ed.; Butterworth: London, 1982.

Sayegh, S. G.; Vera, J. H. Model-Free Methods for Vapor/Liquid Equilibria Calculations. *Chem. Eng. Sci.* **1980**, *35*, 2247−2256.

Smirnova, N. A. *Vestn. Leningr. Univ., Fiz. Khim.* **1959**, 81.

Smith, J. M.; Van Ness, H. C.; Abbott, M. M. *Introduction to Chemical Engineering Thermodynamics*, 5th ed.; McGraw-Hill: New York, 1996; p 88.

Takeo, M.; Nishi, K.; Nitta, T.; Katayama, T. Isothermal Vapor-Liquid Equilibria for Two Binary Mixtures of Heptane with 2-Butanone and 4,4-Methyl-2-Pentanone Measured by a Dynamic Still with a Pressure Regulation. *Fluid Phase Equilib.* **1979**, *3*, 123−131.

Toghiani, R. K.; Toghiani, H.; Venkateswarlu, G. Vapor-Liquid Equilibria for Methyl *tert*-Butyl Ether + Methanol and *tert*-Amyl Methyl Ether + Methanol. *Fluid Phase Equilib.* **1996**, *122*, 157−168.

Tsonopoulos, C. An Emperical Correlation of Second Virial Coefficients. *AIChE J.* **1974**, *20*, 263−272.

Tu, C.-H.; Ou, F.-C. Vapor-Liquid Equilibria of Binary & Ternary Mixtures of 2-Propanol, 1-Chlorobutane, & Acetonitrile at 101.3 kPa. *J. Chem. Eng. Data* **1998**, *43*, 259−263.

Udovenko, V. V.; Fatkulina, L. G. *Zh. Fiz. Khim.* **1952**, *26*, 1439.

Van Ness, H. C. Thermodynamics in the Treatment of Vapor/Liquid Equilibrium (VLE) Data. *Pure Appl. Chem.* **1995**, *67*, 859−872.

Van Ness, H. C.; Abbott, M. M. *Classical Thermodynamics of Non Electrolyte Solutions*; McGraw-Hill: New York, 1982; Chapter 6.

Williamson, A. G. Phase Equilibria of Two-Component Systems. In *Experimental Thermodynamics (Vol. II)*; Le Neindre, B., Vodar, B., Eds.; Butterworth: London, 1975; pp 749−786.

Wolfova, J.; Lineki, J.; Wichterle, I. Vapour-Liquid Equilibrium in the Heptane-2-pentanol and Heptane-2-methyl-1-butanol Systems at 75, 85 and 95 °C. *Fluid Phase Equilib.* **1991**, *64*, 281−289.

Received for review October 4, 1999. Accepted July 10, 2000. We gratefully acknowledge the financial support of the National Science Foundation, Grant CTS-9317812, and the Texas Engineering Experiment Station.

JE9902692